

AMPLIFICATION OF VOLUME REFLECTION BY CRYSTAL AXES

V.V. Tikhomirov

Research Institute for Nuclear Problems, Minsk, Belarus;
e-mail: vvtikh@mail.ru

It is shown that if protons move at small angles with respect to crystal axes which form bent crystal planes the average angle of proton volume reflection from these planes increases several times.

PACS: 61.85.+p, 29.27.Ac, 41.85.Ar

1. INTRODUCTION

Efficient halo cleaning is essential for reaching the maximum LHC luminosity without superconductor magnet damage [1]. For this the proton beam halo scraping by bent crystals can be efficiently used. The possibility of multi-turn proton capture into the planar channeling regime in bent crystals has been studied most extensively [2-4]. The use of "volume reflection" (VR) from bent crystal planes suggested in Ref. [5] causes the most interest at present [4, 6]. Remind that VR manifests themselves in the region of nearly tangential proton motion with respect to (w.r.t.) the bent crystal planes leading to the mean proton beam deflection by the angle of about the critical channeling angle of planar channeling in the direction opposite to that of crystal bent. The reflected beam also increases its angular divergence. The most remarkable advantage of VR is its manifestation in all the angular interval of crystal bending making unnecessary precise crystal-beam alignment.

A correlated particle scattering by atoms forming crystal planes constitute an essence of both methods [2-6]. However, the frequency of collisions of particles with atoms forming crystal axes is about an order higher than that with atoms forming crystal planes. That is why both the amplitude of averaged potential and field strength of crystal axes are nearly an order higher than that of crystal planes. This circumstance puts up a question of using the proton scattering by crystal axes to improve the VR efficiency. We will show that the scattering of protons moving at small angles w.r.t the crystal axes constituting the "reflecting" planes indeed increase the angle of VR.

2. SIMULATION METHOD

To simulate the proton motion in the field of bent crystal axes efficiently we will use an approach combining the ideas of Ref. [7] with the use of axis potential approximation making it possible to evaluate all the proton trajectory characteristics analytically. The essence of the approach [7] is a modification of the classical formulae for the motion in a central field to the case of particle motion in the transverse xy -plain in the cylindrically symmetric "continuum" axial potential $V(\rho)$, $\vec{\rho} = (x, y)$. This motion is characterized by the conserving transverse energy and momentum¹

¹ the system of units in which $\hbar = c = 1$ is used

$$\varepsilon_{\perp} = \varepsilon \frac{v_{\perp}^2}{2} + V(\rho);$$

$$M = \varepsilon [\vec{\rho} \vec{v}_{\perp}]_z = \sqrt{2\varepsilon\varepsilon_{\perp}} b = \varepsilon \rho^2 \frac{d\varphi}{dt}, \quad (1)$$

where ε is the full ultrarelativistic proton energy, b is the collision parameter, φ is the azimuth angle and $\vec{v} = d\vec{\rho}/dt$ is the transverse velocity which radial component

$$v_{\rho} \equiv \frac{d\rho}{dt} = \sqrt{\frac{2}{\varepsilon} [\varepsilon_{\perp} - V(\rho)] - \frac{M^2}{\varepsilon^2 \rho^2}}, \quad (2)$$

allows to evaluate the azimuth deflection angle

$$\varphi(b) = \frac{M}{\varepsilon} \int_{t_i}^{t_f} \frac{dt}{\rho^2} = \frac{M}{\varepsilon} \int_{\rho_i}^{\rho_f} \frac{d\rho}{\rho^2 v_{\rho}(\rho)}, \quad (3)$$

where $\rho_i = \rho(t_i)$ and $\rho_f = \rho(t_f)$ are radial coordinates at the initial (t_i) and final (t_f) instants of proton motion in the field of a particular axis. The sign of the square root in Eq. (2) has to coincide with that of the differential $d\rho$ to make the differential dt positive.

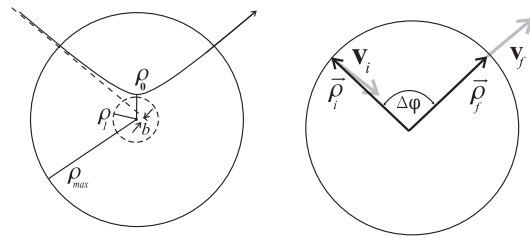


Fig. 1. Proton trajectory and the values $\Delta\varphi, \vec{v}_i, \vec{v}_f, \vec{\rho}_i, \vec{\rho}_f, \rho_{\max}, \rho_0$ and b introduced in the text

A simple form of the axial potential

$$V(\rho) = V_0 \begin{cases} 1 - \rho^2 / 3\rho_1^2, & 0 \leq \rho \leq \rho_1; \\ 2\rho_1 / 3\rho, & \rho_1 \leq \rho \leq \rho_{\max}; \\ 0, & \rho \geq \rho_{\max} \end{cases} \quad (4)$$

allows to treat the proton motion analytically. Note in passing, that a more accurate analytical description is obtained if a proportional to ρ^{-2} contribution is added to $V(\rho)$ in the region $\rho_1 \leq \rho \leq \rho_{\max}$.

We will consider here the case of $\langle 111 \rangle$ Si axes for which $\rho_1 \approx 0.14 \text{ \AA}$ and $V_0 \approx 107 \text{ eV}$. Since the cross sections of these axes constitute a hexagonal lattice in the transverse plain, we will take ρ_{\max} to be equal to half the inter-axis distance $a/2\sqrt{6} \approx 1.109 \text{ \AA}$, where $a \approx 5.431 \text{ \AA}$ is the Si lattice constant.

The values of ρ_i and ρ_f in Eq. (3) can differ from ρ_{\max} in the cases of, respectively, the first axis met by a proton after the entrance through the crystal face and the last one with which the proton interacts before leaving the crystal. In all the other, much more often cases, when a time of proton interaction with an axis is determined solely by the law of motion, one has $\rho_i = \rho_f = \rho_{\max}$ and

$$\varphi(b) = 2 \frac{M}{\varepsilon} \frac{\rho_{\max}}{\rho_0} \int \frac{d\rho}{\rho^2 |v_\rho(\rho)|}, \quad (5)$$

where ρ_0 is the distance of the closest approach to an axis readily obtained using Eq. (4) in the analytical form. Eqs (4) and (5) also allow to obtain the analytical expressions for the azimuth deflection $\Delta\varphi$ angle which allows to evaluate the coordinates

$$\begin{aligned} x_f &= x_i \cos \Delta\varphi + y_i \sin \Delta\varphi, \\ y_f &= y_i \cos \Delta\varphi - x_i \sin \Delta\varphi, \end{aligned} \quad (6)$$

of the transverse position vector $\vec{\rho}_f = (x_f, y_f)$ and the components

$$\begin{aligned} v_x(\rho_f) &= \frac{v_\perp(\rho_f)}{\rho_f} (x_i \cos \Delta\varphi - y_i \sin \Delta\varphi) \\ &\quad - \frac{d\varphi(\rho_f)}{dt} (y_i \cos \Delta\varphi + x_i \sin \Delta\varphi), \\ v_y(\rho_f) &= \frac{v_\perp(\rho_f)}{\rho_f} (y_i \cos \Delta\varphi + x_i \sin \Delta\varphi) \\ &\quad - \frac{d\varphi(\rho_f)}{dt} (x_i \cos \Delta\varphi - y_i \sin \Delta\varphi) \end{aligned} \quad (7)$$

of the transverse velocity $\vec{v}_f = (v_x(\rho_f), v_y(\rho_f))$ at the final moment t_f of the proton interaction with the axis (see Fig. 1).

In order to find the next axis on the proton pass let us introduce the proton position vector

$$\vec{\rho} = \vec{\rho}_f - \vec{a} \quad (8)$$

and collision parameter

$$b = \frac{[\vec{\rho} \vec{v}_f]_z}{v_f} \quad (9)$$

w.r.t. an axis having a position vector \vec{a} in the xy -plain. The desired axis is chosen from the six neighboring ones according to the conditions $|b| < \rho_{\max}$ and $\vec{v}_f \cdot \vec{\rho}_i < 0$. The proton position vector relative to the chosen axis at the moment t'_i when the proton starts to interact with its field is determined then by the formula

$$\vec{\rho}'_i = \vec{\rho} - \frac{\vec{v}_f}{v} \left(\frac{\vec{v}_f \cdot \vec{\rho}}{v} + \sqrt{\rho_{\max}^2 - b^2} \right). \quad (10)$$

A crystal bent with the radius R_b in the xy plane was taken into consideration by the formulae

$$v'_{ix} = v_{fx} + \frac{\Delta z}{R_b}, \quad v'_{iy} = v_{fy} \quad (11)$$

for the components of the transverse velocity $\vec{v}'_i = (v'_{ix}, v'_{iy})$ at the moment t'_i , where

$$\Delta z = \int_{\rho_i}^{\rho_f} \frac{d\rho}{v_\rho(\rho)} \left(\frac{\vec{v}_f \cdot \vec{\rho}}{v} + \sqrt{\rho_{\max}^2 - b^2} \right) \frac{1}{v_f} \quad (12)$$

is the longitudinal path length between the proton consecutive collisions with axes at the momenta t_i and t'_i . The new transverse positions (10) and velocities (11) can be used to simulate consecutive collisions using Eqs. (5)-(7) until the sum $\sum \Delta z$ of the path lengths (12) exceeds the crystal length l_{cr} . When it does, one should put $\sum \Delta z = l_{cr}$ and use Eq. (12) to find the ρ_f value at the moment when the particle leaves the crystal.

When a proton entrance into the crystal is simulated, velocity components are randomly chosen according to both the proton beam divergence and direction while transverse coordinates are chosen completely randomly.

At that if the distances $\rho_i = \sqrt{x_i^2 + y_i^2}$ to all the axes exceed ρ_{\max} , the procedure similar to that described by Eqs. (8)–(12) should be used to evaluate three coordinates and two velocity components at the moment of interaction start at which the proton approaches some axis by the distance $\rho = \rho_{\max}$.

Since an incoherent scattering by nuclei and electrons plays important role in particle deflection by bent crystal axes, we will remind our approach to its simulation which has already allowed to resolve some problem concerning the Landau-Pomeranchuk effect theory [8]. In order to illustrate the idea we will restrict our consideration by the case of scattering by nuclei.

Multiple scattering simulation in logarithmic approximation can be based on the relativistic Coulomb cross section

$$d\sigma = \frac{4Z^2\alpha^2 d\phi d\mathcal{G}}{\varepsilon^2 \mathcal{G}^3} \quad (13)$$

in which Z is an atomic number ($Z=14$ for Si), $\alpha \approx 1/137$, ϕ and \mathcal{G} are the azimuth and polar angles of single proton scattering by a nucleus, respectively. A direct integration of the product $\mathcal{G}^2 d\sigma$ allows to get the average square of the multiple scattering angle per unit length

$$\frac{d\mathcal{G}^2}{dz} = \frac{8\pi Z^2 \alpha^2 n}{\varepsilon^2} \ln \frac{\mathcal{G}_{\max}}{\mathcal{G}_{\min}}, \quad (14)$$

where \mathcal{G}_{\max} and \mathcal{G}_{\min} are, respectively, the minimum and maximum angles taken into consideration and n is the nuclei number density. The local space distribution of nuclei of atoms constituting a crystal axis smeared along its direction is described by the formula

$$n(\rho) = \frac{1}{2\pi u^2 d_{ia}} \exp\left(-\frac{\rho^2}{2u^2}\right), \quad (15)$$

where d_{ia} is the averaged axial inter-atomic distance ($d_{ia} = 4.7 \text{ \AA}$ for $\langle 111 \rangle$ Si axis) and u is the one dimensional root-mean-square amplitude of the nuclei vibrations by equilibria positions. For such a distribution one can take

$$\mathcal{G}_{\min} \approx 1/u\varepsilon \quad (16)$$

in the logarithmic approximation. For \mathcal{G}_{\max} a value $\mathcal{G}_n = 1/R_n\varepsilon$, where R_n is the nucleus radius, is often used, which leads to the well known expression

$$\frac{d\mathcal{G}_{am}^2}{dz} \approx \frac{16\pi Z^2 \alpha^2}{\varepsilon^2} n_0 \ln \frac{183}{Z^{1/3}} \quad (17)$$

for the average square of the multiple scattering angle per unit length in amorphous substance with an atomic number density n_0 .

However if one considers a particle motion at a small angle w.r.t. crystal planes or axes, when the channeling phenomenon plays a crucial role, it would be more adequate to simulate the acts of single scattering by nuclei at angles comparable with the critical channeling angle \mathcal{G}_{ch} individually. For that we usually introduce [8] some boundary angle \mathcal{G}_2 satisfying the condition $\mathcal{G}_{\min} \ll \mathcal{G}_2 \ll \mathcal{G}_{ch}$ and consider the acts of single scattering at angles $\mathcal{G}_{\min} < \mathcal{G} < \mathcal{G}_2$ as a multiple scattering described by Eq. 14, while that at angles $\mathcal{G}_2 < \mathcal{G} < \mathcal{G}_n$ as a single scattering simulated directly with the help of Coulomb cross section (13).

The average square of multiple scattering angle by the nuclei of one crystal axis

$$\mathcal{G}_{ms}^2 = \frac{8\pi Z^2 \alpha^2}{\pi u^2 d_{in} \varepsilon^2} \ln \frac{\mathcal{G}_{\max}}{\mathcal{G}_{\min}} \int_{\rho_0}^{\rho_{\max}} \exp\left(-\frac{\rho^2}{2u^2}\right) \frac{d\rho}{|v_\rho(\rho)|} \quad (18)$$

is obtained by integrating Eqs. (14), (15) along the proton trajectory with the help of the relation $dt = d\rho/v_\rho(\rho)$. Simulation results only slightly depend on the \mathcal{G}_2 value in a considerable region of its choice. We chose it equal to (18).

The proton motion disturbance by the multiple scattering by atoms of one axis is taken into consideration by the velocity component modification according to the equations

$$v_x = v_x + \mathcal{G} \cos \phi, \quad v_y = v_y + \mathcal{G} \sin \phi, \quad (19)$$

where the azimuth angle ϕ is randomly chosen from the interval $(0, 2\pi)$, while the polar one \mathcal{G} can either

be directly taken from Eq. (18) or, more adequately, randomly chosen according to the normal distribution containing (18) as a mean square.

The probability of single proton scattering by the nuclei of atoms constituting one axis is evaluated by the formula

$$P(\mathcal{G}_2 < \mathcal{G} < \mathcal{G}_n) = \frac{4\pi Z^2 \alpha^2}{\pi u^2 d_{in} \varepsilon^2} \left(\frac{1}{\mathcal{G}_2^2} - \frac{1}{\mathcal{G}_n^2} \right) \times \int_{\rho_0}^{\rho_{\max}} \exp\left(-\frac{\rho^2}{2u^2}\right) \frac{d\rho}{|v_\rho(\rho)|}, \quad (20)$$

obtained by integration of the scattering probability $n(\rho)d\sigma$ both over the scattering angles $\mathcal{G}_2 < \mathcal{G} < \mathcal{G}_n$ and along the proton trajectory. The corresponding disturbance of proton motion is simulated using both this probability and Eq. (19) with the polar scattering angle chosen from the interval $(\mathcal{G}_2, \mathcal{G}_n)$ according to the cross section (13). To simplify Eqs. (18) and (20) both the exponent and radial velocity component should be expanded by the point ρ_0 in series and corresponding Gauss integrals should be taken.

The procedure described allows to efficiently simulate a great number (10^5 and more) of trajectories of protons moving through bent crystals at small angles with respect to their axes.

3. SIMULATION RESULTS

Let us consider a set of $\langle 111 \rangle$ crystal axes which constitute vertical crystal planes (1-10) bent in the horizontal plane. Let protons initially move at a small angle θ_0 w.r.t. the latter with the horizontal velocity component being tangent to the bent planes inside the crystal – see Fig. 2.

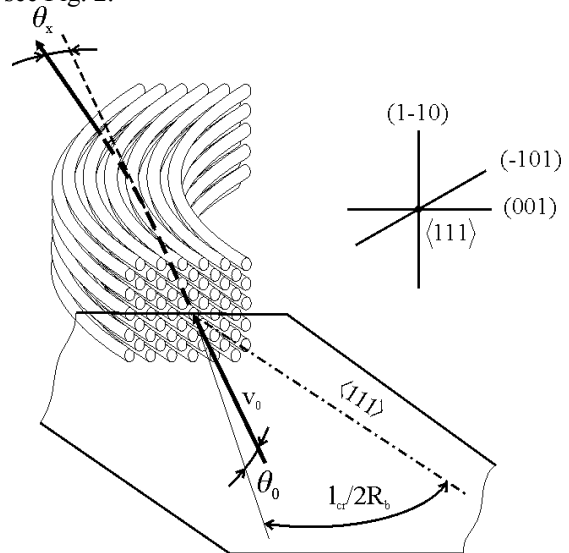


Fig. 2. Proton incidence direction. Protons move at small angle θ_0 w.r.t. crystal axes $\langle 111 \rangle$. Their velocity makes zero angle with the curved planes (1-10) inside the crystal

If the incidence angle θ_0 is sufficiently large the fact that the crystal planes are formed of axes can be

ignored and VR [5] from the bent planes (1-10) has to occur in the region of proton motion at the angles of about the critical channeling angle w.r.t. the bent planes. However if the angle θ_0 is small, the protons will “feel” separate axes in the planes. An impact parameter distribution of the proton scattered by the axes will be random to a degree. For this reason only one can anticipate the increase of the average volume reflection angle as well as of its dispersion. The simulation results confirm this expectation to a much greater extent than would be expected from the estimates, as Fig. 3 demonstrates.

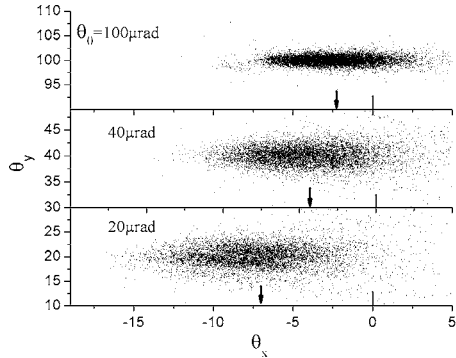


Fig. 3. Proton angular distributions. Indicated by arrows averaged scattering angle $\langle\theta_x\rangle$ increases at small incidence angles θ_0

We will continue to consider the 7 TeV LHC protons as an example. The crystal length l_{cr} and bending radius R_b were equal to 0.5cm and 50m, respectively. Thus, the bending angle θ_b was $l_{cr}/R_b = 100\mu rad$. The protons were initially directed at $50\mu rad = \theta_b/2$ w.r.t. the (1-10) planes and, thus, moved tangentially to them in the region $z \sim l_{cr}/2 = 0.25mm$ inside the crystal. The cases of three incidence angles $\theta_0 = 20, 40$ and $100\mu rad$ were chosen for numerical study.

The last of them allows to neglect the role of axes and observe the usual VR from (1-10) planes. The average deflection scattering angle $\langle\theta_x\rangle$, the angular dispersion $\delta\theta_x$ and the portion P of protons with $\theta_x < 5\mu rad$ turned out to be equal to $-2.3\mu rad$, $2.4\mu rad$ and 98%, respectively.

The opposite case of $\theta_0 = 20\mu rad$ clearly demonstrates the threefold increase of average scattering angle reaching $\langle\theta_x\rangle = -7.1\mu rad$. One also has $\delta\theta_x = 3.6\mu rad$ and $P \approx 94\%$ at $\theta_0 = 20\mu rad$. For the incidence angle $\theta_0 = 40\mu rad$ we obtained $\langle\theta_x\rangle = -4.3\mu rad$, $\delta\theta_x = 3.3\mu rad$ and $P \approx 95\%$. An incomplete selection of the parameters of the geometry of proton interaction with the crystal indicates that even such high $-\langle\theta_x\rangle$ values as $13\mu rad$ are possible.

In order to explicitly demonstrate that the direction of proton deflection in Fig. 3 is opposite to that of the “usual” particle deflection by a bent crystal, we also conducted simulation for the cases of the proton inci-

dence parallel to both crystal planes and axes. The case of proton incidence at zero angle w.r.t. the (1-10) *Si* plane is illustrated by Fig. 4 (as before, protons start to move at the angle $\theta_0 = 20\mu rad$ w.r.t. the $\langle 111 \rangle$ axes). About 66% of protons are captured into the regime of planar channeling and deflected by the angle $\theta_b = 100\mu rad$ of crystal bending into the direction, which is indeed opposite to the deflection direction in Fig. 3.

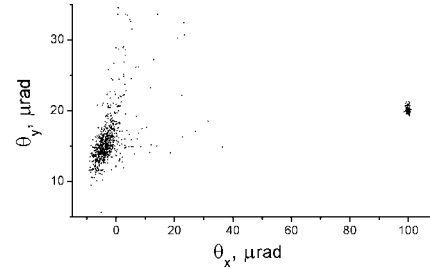


Fig. 4. Distribution of deflection angles θ_x and θ_y under the proton incidence parallel to the (1-10) plane at the angle $\theta_0 = 20\mu rad$ w.r.t. the $\langle 111 \rangle$ axes

The case of proton incidence at zero angle w.r.t. the $\langle 111 \rangle$ axes is illustrated by Fig. 5. The proton deflection direction is again opposite to that in Fig. 3. Fig. 5 also demonstrates specific pattern of proton deflection by strongly bent crystal axes.

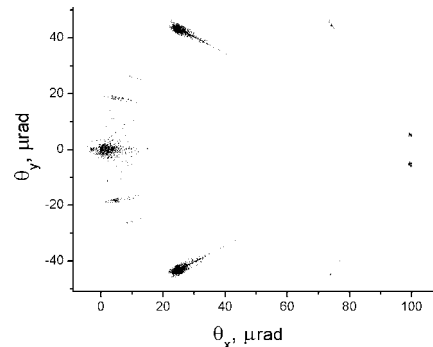


Fig. 5. Distribution of deflection angles θ_x and θ_y under the proton incidence parallel to the $\langle 111 \rangle$ axes

Thus, the direction of proton deflection in Fig. 3 is indeed opposite to that of the usual particle deflection by bent crystal axes and planes and the value of this deflection several times exceeds that of VR from bent crystal planes.

The origin of such an increase of the proton deflection angle becomes clear from Fig. 6 in which the dependence of deflection angles in both transverse directions on the proton pass length is present. Namely, the θ_x dependence on z clearly demonstrates that a large deflection in the horizontal plane is reached because of multiple VRs from several sets of planes.

First of all, when the angle made by the horizontal velocity component with (1-10) planes approaches zero in the region of $z \sim 0.25mm$, a traditional VR from this set of planes occurs which leads to a fast θ_x change by

the value of about the planar channeling angle which is not accompanied by a comparable θ_y change. This is not the case under the similar θ_x changes near $z = 0.07, 0.27$ and 0.38 mm which are accompanied by that of θ_y . Such a *correlated* change of θ_x and θ_y is, most probably, caused by the temporal proton capture to the channeling regime motion by the planes (-101) , $(0-11)$ and others which are neither horizontal nor vertical. Such a multiple VR allows to reach average deflection angles 3...5 times exceeding that of traditional "single" VR.

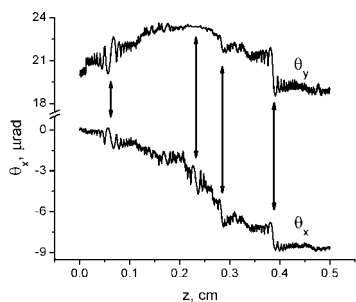


Fig. 6. Proton deflection angles θ_x and θ_y vs its pass length

The angle θ_x evolution of 50 protons illustrated by Fig. 7 demonstrates a common nature of proton deflection by the crystal planes in the several z regions leading to the VR angle increase.

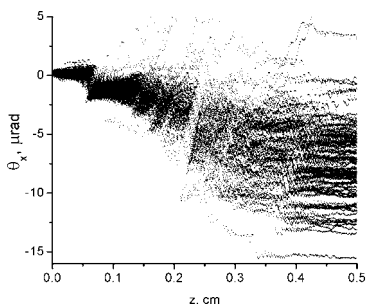


Fig. 7. Proton deflection angle θ_x vs pass length

Thus, our numerical simulations clearly demonstrate a considerable increase of the proton average deflection angle caused by the crystal axes. Both the theory and optimization of the effect will be our further goals.

This work was partly supported by INTAS-CERN grant 03-52-6155. The author is grateful to Prof. X. Artru for the interesting discussions.

REFERENCES

1. V.M. Biryukov, V.N. Chepegin, Y.A. Chesnokov, V. Guidi, W. Scandale. Crystal collimation as an option for the large hadron colliders // *Nucl. Instrum. Meth.* 2005, v. B234, p. 23-30.
2. A.G. Afonin et al. Proton beam extraction from the IHEP accelerator using short silicon crystals // *Phys. Part. Nucl.* 2005, v. 36, p. 21-50.
3. R.A. Carrigan Jr. et al. Beam extraction studies at 900-GeV using a channeling crystal // *Phys. Rev. ST Accel. Beams.* 2002, v. 5, p. 043501-1–043501-24.
4. R.P. Fliller et al. Results of bent crystal channeling and collimation at the Relativistic Heavy Ion Collider // *Phys. Rev.* 2006, v. 9, p. 013501-1–013501-19.
5. A.M. Taratin, S.A. Vorobiev. Volume reflection of high-energy charged particles in quasi-channeling states in bent crystals // *Phys. Lett. A.* 1987, v. 119, p. 425-428.
6. V.M. Biryukov. *Observation of 'volume reflection' effect in crystal collimation experiments:* Preprint physics/0602012.
7. A.I. Akhiezer, N.F. Shulga, V.I. Truten, A.A. Gripenko, V.V. Syshchenko. Dynamics of high-energy charged particles in straight and bent crystals // *Phys. Usp.* 1995, v. 38, p. 1119-1145.
8. V.G. Baryshevsky, V.V. Tikhomirov. The role of incoherent scattering in radiation processes at small angles of incidence of particles on crystallographic axes or planes // *Sov. Phys. JETP.* 1986, v. 63, p. 1116-1123.

УСИЛЕНИЕ ОБЪЕМНОГО ОТРАЖЕНИЯ КРИСТАЛЛИЧЕСКИМИ ОСЯМИ

В.В. Тихомиров

Показано, что при движении протонов под малыми углами к кристаллическим осям, образующим изогнутые плоскости, происходит значительное увеличение среднего угла объемного отражения от этих плоскостей.

ПІДСИЛЕННЯ ОБ'ЄМНОГО ВІДБИТТЯ КРИСТАЛІЧНИМИ ОСЯМИ

В.В. Тихомиров

Показано, що при русі протонів під малими кутами до кристалічних вісей, утворюючих вигнуті площини, має місце значне збільшення середнього кута об'ємного відбиття від цих площин.